OCRbayes: A Bayesian hierarchical modeling framework for Seahorse extracellular flux oxygen consumption rate data analysis

Xiang Zhang[1,2], Taolin Yuan[2], Jaap Keijer[2], Vincent C. J. de Boer[2,*]

1. Theoretical Biology and Bioinformatics, Utrecht University, Padualaan 8, 3584 CH Utrecht, The Netherlands
2. Human and Animal Physiology, Wageningen University, De Elst 1, 6708 WD Wageningen, The Netherlands

Abstract

Mitochondrial dysfunction is involved in many complex diseases. Efficient and accurate evaluation of mitochondrial functionality is crucial for understanding pathology as well as facilitating novel therapeutic developments. As a popular platform, Seahorse extracellular flux (XF) analyzer is widely used for measuring mitochondrial oxygen consumption rate (OCR) in living cells. A hidden feature of Seahorse XF OCR data is that it has a complex data structure, caused by nesting and crossing between measurement cycles, wells and plates. Surprisingly, statistical analysis of Seahorse XF data has not received sufficient attention, and current methods completely ignore the complex data structure, impairing the robustness of statistical inference. To rigorously incorporate the complex structure into data analysis, here we developed a Bayesian hierarchical modeling framework, OCRbayes, and demonstrated its applicability based on analysis of published data sets. We showed that OCRbayes can analyze Seahorse XF OCR experimental data derived from either single or multiple plates. Moreover, OCRbayes has potential to be used for diagnosing patients with mitochondrial diseases.

Introduction

Mitochondria are double-membrane organelles that are central hubs in regulating energy generation and partitioning. Patients with genetic defects in mitochondrial function are often affected by severe and progressive disease in early life.[1] Furthermore, mitochondrial disorders have also been found to be involved in cardiovascular diseases,[2] type II diabetes,[3] neurodegenerative disease[4] and cancer.[5] Thus, restoring mitochondrial function is emerging to be a therapeutic target for both common diseases[6] as well as genetic mitochondrial diseases.[7]

Mitochondria produce energy in oxidative phosphorylation (OXPHOS) primarily by transferring electrons along the electron transport chain (ETC) on the inner membrane. Along the ETC, there are four complexes (complex I, II, III and IV), together building up a proton gradient that is ultimately used by ATP synthase to generate ATP. Since electrons are primarily accepted by O_2 to produce H_2O, the OXPHOS activity can be assessed by measuring oxygen consumption rate (OCR). As a reliable and efficient platform, Seahorse XF analyzer provides a multiwell plate based respirometry assay that is widely used to quantify OCR in living cells.[8] Typically, the Seahorse XF analyzer measures the OCR of cells in a 96-well plate under different ETC/OXPHOS perturbation scenarios, used for assessing mitochondrial functionality such as maximal respiration, leak respiration and ATP-linked respiration.[9]

A typical Seahorse assay includes three measurement cycles for each phase. Every measurement cycle starts by lowering the cartridge and creating a temporary semi-closed ~2 μL chamber.[10] During a measurement cycle, fluorescent oxygen sensors capture oxygen concentration changes in the chamber and outputs OCR. The Seahorse XF analyzer measures OCR in tens to hundreds of thousands of cells per well and typically requires 4—5 replicate wells per experimental group, allowing the analysis of multiple experimental groups in one plate.[11] Since measurement cycles are nested

within phases, phases are crossed with wells, and wells are nested in experimental groups, a very complex structure is inherently embedded in the Seahorse XF OCR data. Surprisingly, current Seahorse XF data analyses most often ignore this complex structure, and by default, data sets are often chopped into subgroups followed by performing ANOVA-like statistical tests. Although there are advanced tools developed for Seahorse data analysis,[12,13] none of them comprehensively take the complexity of the data structure into account. As a result, OCR variation between measurement cycles, replicate wells and replicate plates is overlooked, impairing the robustness of the interpretation of Seahorse XF OCR outcomes, and eventually the development of mitochondrial targeted therapies as well as our understanding of mitochondrial biology.

A natural way to incorporate the complex structure into data analysis is to use hierarchical modeling, which has been extensively developed for analyzing gene expression data.[14,15] Here we developed a Bayesian hierarchical modeling framework, OCRbayes, for the Seahorse XF OCR data analysis. OCRbayes is based on a fully Bayesian approach due to its flexibility and convenience for constructing the hierarchical models. To demonstrate the applicability of our approach as well as its potential implication for mitochondrial disease diagnostics, we applied OCRbayes to a publicly available OCR data set,[13] which contains over 200 Seahorse experiments performed on human fibroblasts derived from patients with mitochondrial diseases and controls.

Method

OCRbayes: A Bayesian hierarchical modeling framework for Seahorse OCR data analysis

In order to incorporate the complex data structure into the analysis of Seahorse XF OCR measurements, we developed a Bayesian hierarchical modeling framework, OCRbayes. In this study, we focused on experimental data

containing two groups, such as patient and control group. From our perspective, the Seahorse OCR data include three levels, including 1) measurement cycle, 2) well and 3) plate.

During a measurement cycle, fluorescent oxygen sensors capture oxygen concentration changes in the chamber and outputs OCR. For every interval, multiple measurement cycles are performed in order to accurately measure the OCR. A typical Seahorse assay contains four intervals. The first interval refers to initial phase, and the second, third, fourth interval refer to phase after injecting oligomycin (blocking proton translocation through ATP synthase), FCCP (allowing protons to move into the mitochondrial matrix independent of the ATP synthase) and antimycin/rotenone (inhibiting complex I and III, shutting down mitochondrial respiration).
The variation between the OCR values within an interval is the between measurement cycle variation. Since OCR values must be positive, we used a lognormal distribution with the true OCR value at the log scale ($\log OCR_{true}$) and the between measurement cycle standard deviation (also at the log scale, $\log OCR_{sd}$) to model each observed OCR value (OCR_{obs}).

$$OCR_{obs}[i] \sim \text{Lognormal}(\log OCR_{true}[P[i],W[i],I[i]], \log OCR_{se}[P[i],I[i]]) \quad (1)$$

OCR_{obs} is a vector of length $N_{plate} \times N_{well} \times N_{interval} \times N_{measurement}$, where N_{plate}, N_{well}, $N_{interval}$ and $N_{measurement}$ are number of plates, wells, intervals and measurement cycles, respectively. The $\log OCR_{true}$ refers to N_{plate} layers of matrices. Each layer is a matrix with N_{well} rows and $N_{interval}$ columns. $\log OCR_{sd}$ is a matrix of N_{plate} rows and $N_{interval}$ columns.

In a typical Seahorse XF assay, one cell line undergoing the same experimental treatment is seeded in multiple wells. However, the OCRs in these replicate wells will not be the same, and the difference is called between well variation. One obvious reason causing the between well variation is that the number of cells in these replicate wells are not identical. To adjust for the effect of cell number difference, we modeled the

true OCR value as a function of the cell number, and from there estimated $OCR_{per\ 1k\ cells}$, which represents OCR value per 1000 cells that received the same treatment (or from the same group) and injection. In addition to cell number difference, technical, procedural or instrumental noise can also contribute to between well variation. We captured this well-to-well variation after accounting for cell number difference with the residual parameter σ_{well}.

$$\log OCR_{true}[P[i],W[i],I[i]] \sim Normal(OCR_{per\ 1k\ cells}[P[i],G[i],I[i]] \times N_{cells}[W[i]], \sigma_{well}[P[i],G[i],I[i]]) \quad (2)$$

$OCR_{per\ 1k\ cells}$ is a three-dimensional matrix with N_{plate} layers, and each layer has N_{group} rows and $N_{Interval}$ columns. N_{cells} is a vector of length N_{well}, and every entry represents the cell number in that well.

Apart from the technical replicates in one plate, the biological insight for a (patient) cell line or a specific condition is generally validated by repeating the Seahorse assay on different days. As a result, OCR data are distributed on more than one plate. Due to batch effects such as plating, culturing or environmental differences between time and laboratories, OCR measurements will differ between plates. To take into account the between plate variation, we used another lognormal distribution with the logarithm transformed OCR value per 1000 cells, ($\mu_{OCR_{per\ 1k\ cells}}$) and the between plate standard deviation (σ_{plate}) to model the OCR value per 1000 cells $OCR_{per\ 1k\ cells}$.

$$OCR_{per\ 1k\ cells}[P[i],G[i],I[i]] \sim Lognormal(\log(\mu_{OCR_{per\ 1k\ cells}}[G[i], I[i]]), \sigma_{plate}[G[i], I[i]]) \quad (3)$$

Bayesian inference

OCRbayes focuses on calculating posterior distributions for OCR per 1000 cells in various experimental conditions ($P(\mu_{OCR_{per\ 1k\ cells}} | OCR_{obs})$). The

posterior distributions were combinations of prior distributions ($P(\log OCR_{se})$, $P(\sigma_{well})$, $P(\sigma_{plate})$ and $P(\mu_{OCR_{per\ 1k\ cells}})$), and the likelihood function ($P(OCR_{obs}|N_{cell}, \mu_{OCR_{per\ 1k\ cells}}, \log OCR_{sd}, \sigma_{well}, \sigma_{plate})$)

In this study, since our case studies focused on human fibroblast cells, we used informative prior distributions for $\log OCR_{sd}$, σ_{well}, σ_{plate} and $\mu_{OCR_{per\ 1k\ cells}}$. Since values of all these parameters must be positive, we used four lognormal distributions. We applied maximum likelihood estimation to calculate the lognormal distribution parameters based on the Seahorse XF OCR data in OCR-stats[13] by running the fitdistr function built in the MASS r package. In this study, our prior distributions are

$$\begin{aligned} \log OCR_{sd} &\sim \text{Lognormal}(-3.23, 0.79) \\ \sigma_{well} &\sim \text{Lognormal}(-1.62, 0.53) \\ \sigma_{plate} &\sim \text{Lognormal}(-1.18, 0.05) \\ \mu_{OCR_{per\ 1k\ cells}} &\sim \text{Lognormal}(0.3, 0.79) \end{aligned}$$

The Bayesian multi-level model of OCRbayes was implemented in Stan (version 2.19.3).[16] We fitted the model by running Hamiltonian Markov Chain Monte Carlo. We ran four Markov chains with 2000 iterations in each chain. The codes can be found at https://github.com/XiangZhangSC/seahorse.

Calculation of bioenergetic measures

Based on OCR (per 1000 cells), we calculated various bioenergetic measures, such as basal respiration, proton leak, ATP-linked respiration, spare respiratory capacity and maximal respiration. These bioenergetic measures are defined as below.

$$\text{Basal respiration} = OCR_{per\ 1k\ cells,\ initial} - OCR_{per\ 1k\ cells,\ antimycin/rotenone} \quad (4)$$

$$\text{ATP-linked respiration} = OCR_{per\ 1k\ cells,\ initial} - OCR_{per\ 1k\ cells,\ oligomycin} \quad (5)$$

$$\text{Proton leak} = OCR_{per\ 1k\ cells,\ oligomycin} - OCR_{per\ 1k\ cells,\ antimycin/rotenone} \quad (6)$$

$$\text{Spare respiratory capacity} = OCR_{per\ 1k\ cells,\ FCCP} - OCR_{per\ 1k\ cells,\ initial} \quad (7)$$

$$\text{Maximal respiration} = OCR_{per\ 1k\ cells,\ FCCP} - OCR_{per\ 1k\ cells,\ antimycin/rotenone} \quad (8)$$

Human fibroblast OCR data

To benchmark OCRbayes as well as illustrate how OCRbayes can be used for analyzing OCR in patients with mitochondrial diseases, we used the OCR data set provided in Yepez et al. [13]. This data set contains Seahorse OCR measurements from 203 human fibroblast cell lines that have been assayed in 126 plates. Normal human dermal fibroblast (NHDF) reference cell lines were used as controls in all plates. The other 202 cell lines were derived from patients suspected to suffer from rare mitochondrial diseases. Among these 202 cell lines, 26 fibroblast cell lines were measured in multiple plates. We used the 176 patient fibroblast cell lines that were assayed in a single plate as well as the control cell line in the same plates for estimating prior distributions. The other 26 fibroblast cell lines were used for benchmarking OCRbayes. Among the 202 cell lines that were analyzed, Yepez et al. [13] labeled 6 patient cell lines as positive controls that have shown statistically significant reduction in maximum respiration. Meanwhile, Yepez et al. also labeled another two patient cell lines as negative controls, since these cell lines did not show changes in OCR in earlier experiments.[13]

We processed the original data by removing wells in which single or more OCR measurements were missing. After filtering, we used 176 patient cell lines together with the NHDF control cell line on 78 plates for estimating the prior distributions for between measurement cycle variation ($\log OCR_{sd}$) and between well variation (σ_{well}). To estimate the prior distribution for between plate variation (σ_{plate}) and mean OCR per 1000 cells ($\mu_{OCR_{per\ 1k\ cells}}$), we used the OCR values from the NHDF cell lines that were plated in all 78 plates.

Statistical analysis

For benchmarking OCRbayes, we compared the patient cell lines to the control cell line (NHDF). Since mitochondrial dysfunction is often reflected in the

maximal respiration, which was also evaluated previously in the Yepez et al. study,[13] we reported here the mean log2 fold change of maximal respiration together with the False Discovery Rate (FDR). FDR was calculated based on the posterior error probability ($1 - \mathrm{P}(\log_2(\frac{\text{patient}}{\text{control}} | \mathrm{OCR}_{obs}) < 0)$), where $\mathrm{P}(\log_2(\frac{\text{patient}}{\text{control}} | \mathrm{OCR}_{obs})$ represented the posterior distribution of fold change after fitting the Bayesian model to the experimental OCR data. If the FDR was below 0.05, we considered that the difference between patient and control cell line was statistically significant.

Results

OCRbayes: from OCR to respiration metric difference

To demonstrate the applicability, we applied OCRbayes to analyze OCR data derived from two patient cell lines with known mutations in either *BOLA3* or *PET100* gene. These two genes encode proteins that are essential for biogenesis or assembly of mitochondrial complexes.[17–19] We compared the patient cell line to the control cell lines within their respective plates. These two cell lines were both assayed on two plates on two different days. For both cell lines, we observed a clear decrease in maximal respiration compared to the control cell lines in both plates (Figure 1A and 1E). Meanwhile, we noticed that the range of OCR values in the two plates used for profiling *BOLA3* patient cell line differed considerably (Figure 1A). In particular, maximal OCR value in the first plate was around 200 pmol/min, whereas in the second plate the maximal OCR value was around 100 pmol/min. In contrast, the range of OCR values in the two plates used for profiling *PET100* were similar to each other. In addition, it was obvious that there was considerable variation between the replicate wells in both plates for both cell lines.

By applying OCRbayes, we combined the two plates for each cell line, calculated the posterior distributions for OCR per 1000 cells during the four intervals of a typical Seahorse assay, including initial phase without injection (Int1), oligomycin phase (Int2), FCCP phase (Int3) and antimycin/rotenone phase (Int4) (Figure 1B and 1F). Next, the calculated posterior OCR per 1000 cells for the four intervals were transformed into the various respiration metrics, including ATP-linked respiration, basal respiration, maximal respiration, proton leak and spare respiratory capacity (Figure 1C and 1G). In the last step, we compared the respiration metrics in patient cell line to the control cell line, and calculated the posterior distribution for log2(fold change) (Figure 1D and 1H). We observed that *BOLA3* patient cell line showed reduction in basal respiration (posterior mean log2(fold change) -0.974, 95% credible interval [-1.93, -0.0970]) and maximal respiration (-1.06 [-1.87,-0.228]), compared to the control cell line (Figure 1D). On the other hand, we observed no difference in ATP-linked respiration (-1.08 [-2.38, 0.117]), proton leak (-0.630 [-3.87, 2.32]) and spare respiratory capacity (-1.26 [-4.41,1.62]) between *BOLA3* patient cell line and the control cell line (Figure 1D). Meanwhile we observed lower ATP-basal respiration (-1.75 [-3.18, -0.546]), basal respiration (-1.58 [-2.52, -0.667]) and maximal respiration (-1.28 [-2.10, -0.436]) in the *PET100* patient cell line than the control cell line (Figure 1H). We observed no difference in proton leak (-0.906 [-4.14,2.54]) and spare respiratory capacity (-0.826 [-3.29, 2.34]) in the *PET100* patient cell line compared to the control cell line (Figure 1H).

OCRbayes accounts for various technical variations during Seahorse XF OCR data analysis

OCR measurements generated by the Seahorse XF analyzer were affected by various technical variations, including between measurement cycle variation, between well variation and between plate variation. To visualize

237 the technical variations, we used the cell line with a genetic mutation in
238 *NSUN3* gene (patient cell line 76065). This cell line was measured on five
239 different plates, allowing us to visualize all three technical variations.

240 OCRbayes calculated the between measurement cycle variation for each plate
241 during each interval. For each cell line in each plate, OCRbayes calculated
242 the between well variation during each interval. Regarding the between plate
243 variation, OCRbayes estimated it for each cell line during each interval.
244 All the variation values were on the log scale. We observed that for both
245 patient and control cell line in the initial phase (Int1) and FCCP phase
246 (Int3), the between plate variation was larger than the between well
247 variation, which itself was larger than the between measurement cycle
248 variations (Figure 2). However, in the oligomycin phase (Int2) and
249 antimycin/rotenone phase (Int4), the between plate variation was not always
250 larger than the other two technical variations (Figure 2). In particular, we
251 observed that the between well variation was larger than the between
252 measurement cycle and the between plate variation in three plates during the
253 antimycin/rotenone phase (Int4) in the patient cell line.

254 Benchmark OCRbayes

255 To demonstrate that OCRbayes works properly, we applied it to analyze the
256 published Seahorse XF OCR data set containing 26 patient cell lines as well
257 as a control cell line reported by Yepez et al. [13]. This data set contains 6
258 cell lines that were labeled as positive controls and 2 cell lines that were
259 labeled as negative controls (as explained in the material and methods
260 section).

261 Based on our analysis, we found 6 patient cell lines that had lower maximal
262 respiration compared to the control cell line with False Discovery Rate (FDR)
263 below 0.05 (Figure 3A and B). Among the 6 patient cell lines that showed
264 statistically significant reduction in maximal respiration compared to the
265 control cell line, the patient cell line 73387 (mutation in *PET100* gene)

266 showed the largest effect whereas the patient cell line 76065 (mutation in
267 *NUSN3* gene) showed the smallest effect (Figure 3A). Five of these 6 patient
268 cell lines were labeled as positive controls in the original study.[13]
269 Meanwhile, the two negative controls (patient cell lines 73901 and 91410)
270 had FDR above 0.05 in our analysis.

271 Our analysis successfully recalled both negative controls and five out of
272 six positive controls. Interestingly, our analysis showed that there was no
273 significant reduction of maximal respiration in the cell line with a genetic
274 mutation in *SFXN4* gene (patient 61818) that was previously labeled as
275 positive control.[13] This patient cell line was measured on three independent
276 plates on three different days. The range of OCR values of these three plates
277 differed, indicating considerable between plate variation (Figure 4A). The
278 OCR profiles of the patient and control cell line were overlapping in the
279 first plate (Figure 4A). In contrast, the OCR profiles derived from the
280 second and third plate showed OCR decreasing in the patient cell line
281 compared to the control cell line, especially during the FCCP phase (Figure
282 4A). Meanwhile, we observed considerable variation between the replicate
283 wells as well as measurement cycles in these Seahorse assays (Figure 4A).
284 In addition, the between measurement cycle variation in the third plate
285 seemed to be larger than the other two plates (Figure 4A). We analyzed these
286 three repeated experiments separately as well as combined them together. Our
287 separate analysis showed that none of the three experiments showed
288 significant reduction in maximal respiration in the *SFXN4* patient cell line
289 (Figure 4B). The posterior mean log2(fold change) and the corresponding 95%
290 credible intervals derived from the first, second and third Seahorse assay
291 were 0.122 [-0.834, 1.04], -0.431 [-1.40, 0.499] and -0.0977 [-1.04,
292 0.827], respectively. When we used OCRbayes to analyze all the three plates
293 together, we found that the posterior mean log2(fold change) of maximal
294 respiration was -0.200 [-0.877, 0.500] compared to the control cell line

295 (Figure 4C). However, this tendency of reduction in maximal respiration in
296 *SFXN4* patient cell line was not statistically significant.

297 OCRbayes can be used to evaluate the probability that a 298 patient fibroblast cell line has an abnormality in 299 mitochondrial respiration.

300 A feature that makes OCRbayes unique from other methods is that OCRbayes can
301 evaluate what is the probability that a patient has abnormality in his or
302 her fibroblast mitochondrial respiration based on a single Seahorse assay
303 or multiple Seahorse assays. To demonstrate this feature, we used two
304 patient cell lines that showed significant reduction in maximal respiration
305 in our analysis. One patient cell line was the *PET100* gene mutation
306 fibroblast (patient cell line 73387) and the other patient cell line was
307 *NSUN3* gene mutation fibroblast (patient cell line 76065). Among the 6
308 patient cell lines that showed statistically significant reduction in
309 maximal respiration compared to the control cell line, the *PET100* and *NSUN3*
310 cell line showed the largest and smallest effect, respectively (Figure 3B).

311 The *PET100* patient cell line was measured on two plates. Based on the first
312 assay, our analysis showed that the posterior probability of this *PET100*
313 mutation carrier having lower maximal respiration than the control was
314 97.8%. By repeating the experiment once more, the posterior probability
315 increased to 99.8% (Figure 5A). In contrast, the cell line with mutation in
316 *NSUN3* gene (patient cell line 76065) was measured on five different plates.
317 Our analysis showed that based on the first assay, the posterior probability
318 of this *NSUN3* mutation carrier having lower maximal respiration than the
319 control was 41.3%. Repeating the assay once increased the posterior
320 probability from 41.3% to 73.4%. When the assay was repeated for the third,
321 fourth and fifth time, the corresponding posterior probabilities increased
322 to 78.7%, 87.7% and 90.0%, respectively (Figure 5B). In summary, we
323 demonstrate that OCRbayes can be used to evaluate the probability that a

patient fibroblast cell line has an abnormality in mitochondrial respiration based on a single Seahorse assay or multiple Seahorse assays.

Discussion

Although Seahorse XF analyzer is widely used in bioenergetic profiling, its data analysis has not received sufficient attention. A hidden feature of Seahorse XF OCR data is that it contains a complex data structure. The complex data structure is due to the fact that measurement cycles are nested within injections, injections are crossed with wells, and wells are nested in plates. As far as we know, currently there is no data analysis protocol that takes into account this complex data structure, impairing the robustness of Seahorse XF OCR data analysis outcomes. This is because when one ignores the data structure, one also ignores the variations between measurement cycles, between wells and between plates. In order to make the Seahorse data analysis more robust, in this study we developed a Bayesian hierarchical modeling approach, OCRbayes, which accounts for all these technical variations during the data analysis.

Seahorse XF OCR measurements are noisy

An OCR value is determined not only by mitochondrial activity, but also by technical noise including 1) between measurement cycle variation, 2) between well variation and 3) between plate variation.

Every phase typically contains three measurement cycles, resulting in three OCR values. Since every measurement cycle starts with a "mix and wait" step to ensure the same baseline of cell values, cell physiology should not substantially change within a phase. Existing tools such as OCR-stats[13] and SHORE[12] use different strategies to select a single data point to represent an injection phase. When different data points were chosen, one can get different outcomes, making the current Seahorse XF data analysis less robust.

351 To avoid this ambiguity, our approach did not select any particular data
352 point, instead modeled all three OCR data. By doing so, we incorporated the
353 uncertainty about "which data point should I choose?" into the data
354 analysis and focused on the average behavior.

355 The between well variation refers to a common observation that OCR values
356 differ among the replicate wells. One important factor leading to the
357 variation between replicate wells is that cell numbers are not identical in
358 these wells. The wells with more cells would have higher OCR than the wells
359 containing fewer cells. Fortunately, cell number in each well can be
360 quantified experimentally and used for the data analysis.[20,21] In addition to
361 cell number difference, initial conditions, treatment concentration, or
362 fluorophore sleeve calibration can also contribute to variation between
363 wells. OCRbayes also takes into account the between well variation caused by
364 these unobserved factors.

365 Between plate variation takes place when the same Seahorse experiment is
366 repeated on different days and on more than one plate. Due to differences in
367 temperature, seeding time, growth time, growth medium, sensor cartridge as
368 well as treatment efficiency, the OCR outcomes will differ between
369 plates.[13,22] Often the between plate variation is assumed to be the dominant
370 technical variation involved in Seahorse OCR data. Based on our analysis, we
371 showed that this assumption may be appropriate for OCR measurements derived
372 from the initial and FCCP phase, but may not work for the OCR values derived
373 from oligomycin and antimycin/rotenone phase. OCR values in the oligomycin
374 and antimycin/rotenone phase were very small and possibly close to the
375 detection limit of the Seahorse XF in a well. Thus, it is more challenging to
376 accurately measure the OCR in these phases.

Comparison with other statistical tool for Seahorse XF OCR data analysis

In this work, we compared the maximal respiration in 26 patient cell lines to the control cell line individually as what was done in OCR-stats.[13] Overall our analysis recalled successfully all negative controls and five out of six positive controls. Patient cell line 61818 was labeled as a positive control since this patient was found having a mutation in *SFXN4* gene. A recent study based on erythroleukemic cell line showed that *SFXN4* knockout resulted in significant decrease in all parameters of respiration, including baseline respiration, respiratory ATP synthesis, maximal respiration, and spare respiratory capacity.[23] However, our analysis showed that the maximal respiration of this patient was not significantly different from the control cell line. Our further analysis showed that the patient cell line only showed a tendency of having lower maximal respiration than control in one of the three repeated experiments.

We also noticed that other outcomes were also not identical as what was presented in the OCR-Stats publication.[13] Strikingly, in our analysis *PET100* mutation fibroblast (patient cell line 73387) showed a significant decrease in maximal respiration compared to the control cell line. However, in the OCR-stats,[13] the difference in maximal respiration was not statistically significant in this patient. This patient was diagnosed carrying a homozygous loss of function mutation in the *PET100* gene, which encodes a mitochondrial complex IV biogenesis factor.[13,17,18] A homozygous truncating variant (c.142C|T, p.(Gln48*)) in the *PET100* gene was found to lead to a complete loss of enzyme activity, and caused deficiency in complex IV.[24] Therefore, our observation of significant reduction in maximal respiration in *PET100* mutation fibroblast based on the OCRbayes is in line with the observed loss of enzymatic activity in patients carrying the genetic mutations in *PET100*. This difference in analysis outcome highlighted the advantage of OCRbayes which used hierarchical models to

incorporate the complex data structure into Seahorse OCR data analysis, helping separate the technical variations from the OCR measurements and identify difference in the biological OCR.

OCRbayes is potentially used for screening patients with mitochondrial diseases

Since an increase in proton leak or a decrease in basal or maximal respiration are indicators of mitochondrial dysfunction,[25] Seahorse XF is potentially to be used for screening mitochondrial disease patients. Besides providing solely statistical significance information as other methods do, OCRbayes allows us to calculate posterior probability that the maximal respiration (or any other respiration metrics) was abnormal in a patient even based on a single Seahorse assay. This feature is also helpful for deciding whether we need to run a single or multiple Seahorse assays for a patient.

For example, the patient cell line with mutation in *PET100* gene showed the largest decrease in maximal respiration in our analysis. The posterior probability for this patient having abnormal mitochondrial respiration after observing a single Seahorse assay was already about 98%. It is reasonable to run just a single assay in this case. In contrast, the cell line with mutation in *NSUN3* gene had the smallest effect size among all the patient cell lines that showed significant reduction in maximal respiration. The posterior probability of this patient having impaired maximum respiration after running a single Seahorse assay was modest (about 40%). Repeating the experiment once more increased the posterior probability from 40% to 70%. Thus in this case, it is beneficial to run multiple Seahorse assays. We think that the posterior probability is a useful metric to help scientists to decide whether to perform extra Seahorse assays on the patient cell lines. The ability of posterior probability calculation by OCRbayes not only allows to make better conclusions about the significance of the effect of the experimental perturbation, it can also prevent from repeating

437 unnecessary, often expensive, experiments. Furthermore, when the
438 availability of patient material or the number of target cells (specific
439 isolated immune cell subsets) is limited, OCRbayes is valuable to exploit
440 the limited data and facilitate proper validation the experiments.

441 Strengths and limitations

442 OCRbayes has several advantages. The first advantage of our approach is that
443 it incorporates various technical variations including between measurement
444 cycle variation, between well variation as well as between plate variation
445 during the estimation of bioenergetic measures. All current methods need to
446 choose a single data point from the three measurement cycles to represent
447 the OCR during a particular phase. This procedure ignores the uncertainty
448 and makes analysis less robust because different choice of data points may
449 lead to different results. The second advantage is that OCRbayes can
450 calculate posterior probability for difference in various bioenergetic
451 measures based on Seahorse OCR data consisting of a single plate or multiple
452 plates. This is a useful feature for screening samples derived from patients
453 with mitochondrial diseases.

454 One limitation of this study is that OCRbayes currently focused on human
455 fibroblasts cell lines. This is because our model development was restricted
456 to the limited publicly available Seahorse OCR data sets. In the future,
457 OCRbayes can be extended to other cell types when more experimental data are
458 collected and combined to establish databases with experimental OCR data.

459 Data Availability

460 The dataset supporting the conclusions of this article is included within
461 the article and its additional file.

462 ## Author contributions

463 XZ developed the OCRbayes and wrote the manuscript. TY and JK contributed to
464 the conceptualization of the project and edited the manuscript. VB
465 supervised the project and edited the manuscript. All authors read and
466 approved the final manuscript.

467 ## Competing interests

468 The authors declare that they have no competing interests

469 ## Reference

470 1. Koene, S. *et al.* Developing outcome measures for pediatric mitochondrial
471 disorders: which complaints and limitations are most burdensome to patients
472 and their parents? *Mitochondrion* **13**, 15—24 (2013).

473 2. Ballinger, S. W. Mitochondrial dysfunction in cardiovascular disease. *Free*
474 *Radic. Biol. Med.* **38**, 1278—95 (2005).

475 3. Szendroedi, J., Phielix, E. & Roden, M. The role of mitochondria in insulin
476 resistance and type 2 diabetes mellitus. *Nat. Rev. Endocrinol.* **8**, 92—103
477 (2011).

478 4. Johri, A. & Beal, M. F. Mitochondrial dysfunction in neurodegenerative
479 diseases. *J. Pharmacol. Exp. Ther.* **342**, 619—30 (2012).

480 5. Erez, A. & DeBerardinis, R. J. Metabolic dysregulation in monogenic
481 disorders and cancer – finding method in madness. *Nat. Rev. Cancer* **15**, 440—
482 8 (2015).

483 6. Murphy, M. P. & Hartley, R. C. Mitochondria as a therapeutic target for
484 common pathologies. *Nat. Rev. Drug Discov.* **17**, 865—886 (2018).

485 7. Weissig, V. Drug Development for the Therapy of Mitochondrial Diseases.
486 *Trends Mol. Med.* **26**, 40—57 (2020).

487 8. Wu, M. *et al.* Multiparameter metabolic analysis reveals a close link
488 between attenuated mitochondrial bioenergetic function and enhanced
489 glycolysis dependency in human tumor cells. *Am. J. Physiol. Cell Physiol.* **292**,
490 C125—36 (2007).

491 9. Chacko, B. K. *et al.* The Bioenergetic Health Index: a new concept in
492 mitochondrial translational research. *Clin. Sci. (Lond).* **127**, 367—73
493 (2014).

494 10. Gerencser, A. A. *et al.* Quantitative microplate-based respirometry with
495 correction for oxygen diffusion. *Anal. Chem.* **81**, 6868—78 (2009).

496 11. Artyomov, M. N. & Van den Bossche, J. Immunometabolism in the Single-Cell
497 Era. *Cell Metab.* **0**, (2020).

498 12. Nicholas, D. *et al.* Advances in the quantification of mitochondrial
499 function in primary human immune cells through extracellular flux analysis.
500 *PLoS One* **12**, e0170975 (2017).

501 13. Yépez, V. A. *et al.* OCR-Stats: Robust estimation and statistical testing
502 of mitochondrial respiration activities using Seahorse XF Analyzer. *PLoS*
503 *One* **13**, e0199938 (2018).

504 14. Robinson, M. D., McCarthy, D. J. & Smyth, G. K. edgeR: a Bioconductor package
505 for differential expression analysis of digital gene expression data.
506 *Bioinformatics* **26**, 139—40 (2010).

507 15. Love, M. I., Huber, W. & Anders, S. Moderated estimation of fold change and
508 dispersion for RNA-seq data with DESeq2. *Genome Biol.* **15**, 550 (2014).

509 16. Carpenter, B. *et al.* Stan : A Probabilistic Programming Language. *J. Stat.*
510 *Softw.* **76**, (2017).

511 17. Oláhová, M. *et al.* LRPPRC mutations cause early-onset multisystem
512 mitochondrial disease outside of the French-Canadian population. *Brain* **138**,
513 3503—19 (2015).

514 18. Lim, S. C. *et al.* A founder mutation in PET100 causes isolated complex IV
515 deficiency in Lebanese individuals with Leigh syndrome. *Am. J. Hum. Genet.* **94**,
516 209—22 (2014).

517 19. Haack, T. B. *et al.* Homozygous missense mutation in BOLA3 causes multiple
518 mitochondrial dysfunctions syndrome in two siblings. *J. Inherit. Metab. Dis.*
519 **36**, 55—62 (2013).

520 20. Little, A. C. *et al.* High-content fluorescence imaging with the metabolic
521 flux assay reveals insights into mitochondrial properties and functions.
522 *Commun. Biol.* **3**, 1—10 (2020).

523 21. Janssen, J. J. E. *et al.* Novel standardized method for extracellular flux
524 analysis of oxidative and glycolytic metabolism in peripheral blood
525 mononuclear cells. *Sci. Rep.* **11**, 1662 (2021).

526 22. Koopman, M. *et al.* A screening-based platform for the assessment of
527 cellular respiration in Caenorhabditis elegans. *Nat. Protoc.* **11**, 1798—816
528 (2016).

529 23. Paul, B. T., Tesfay, L., Winkler, C. R., Torti, F. M. & Torti, S. V.
530 Sideroflexin 4 affects Fe-S cluster biogenesis, iron metabolism,
531 mitochondrial respiration and heme biosynthetic enzymes. *Sci. Rep.* **9**, 19634
532 (2019).

533 24. Oláhová, M. *et al.* A truncating PET100 variant causing fatal infantile
534 lactic acidosis and isolated cytochrome c oxidase deficiency. *Eur. J. Hum.*
535 *Genet.* **23**, 935—9 (2015).

536 25. Brand, M. D. & Nicholls, D. G. Assessing mitochondrial dysfunction in
537 cells. *Biochem. J.* **435**, 297—312 (2011).

Figures

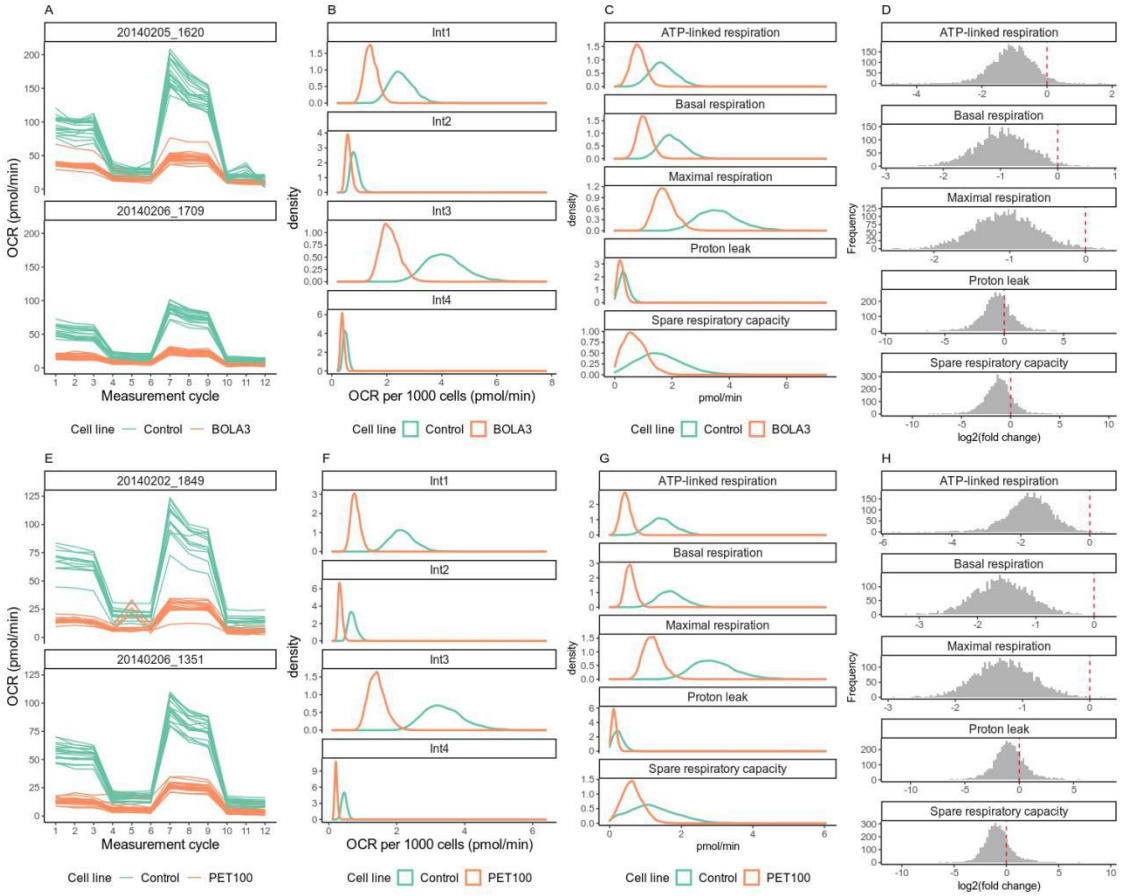

Figure 1 (A) and (E) are OCR profiles for patient cell lines that have a genetic mutation in either BOLA3 (A) or PET100 (E), compared to control cell lines in two plates. (B) and (F) are posterior distributions for OCR per 1000 cells in BOLA3 (B) and PET100 (F) mutated patient cell lines during initial phase (Int1), oligomycin phase (Int2), FCCP phase (Int3) and antimycin/rotenone phase (Int4). (C) and (G) are posterior distributions for respiration metrics in BOLA3 (C) and PET100 (G) mutated patient cell lines and control cell lines. (D) and (H) are posterior distributions of log2 fold change in the respiration metrics between patient and control cell line.

551

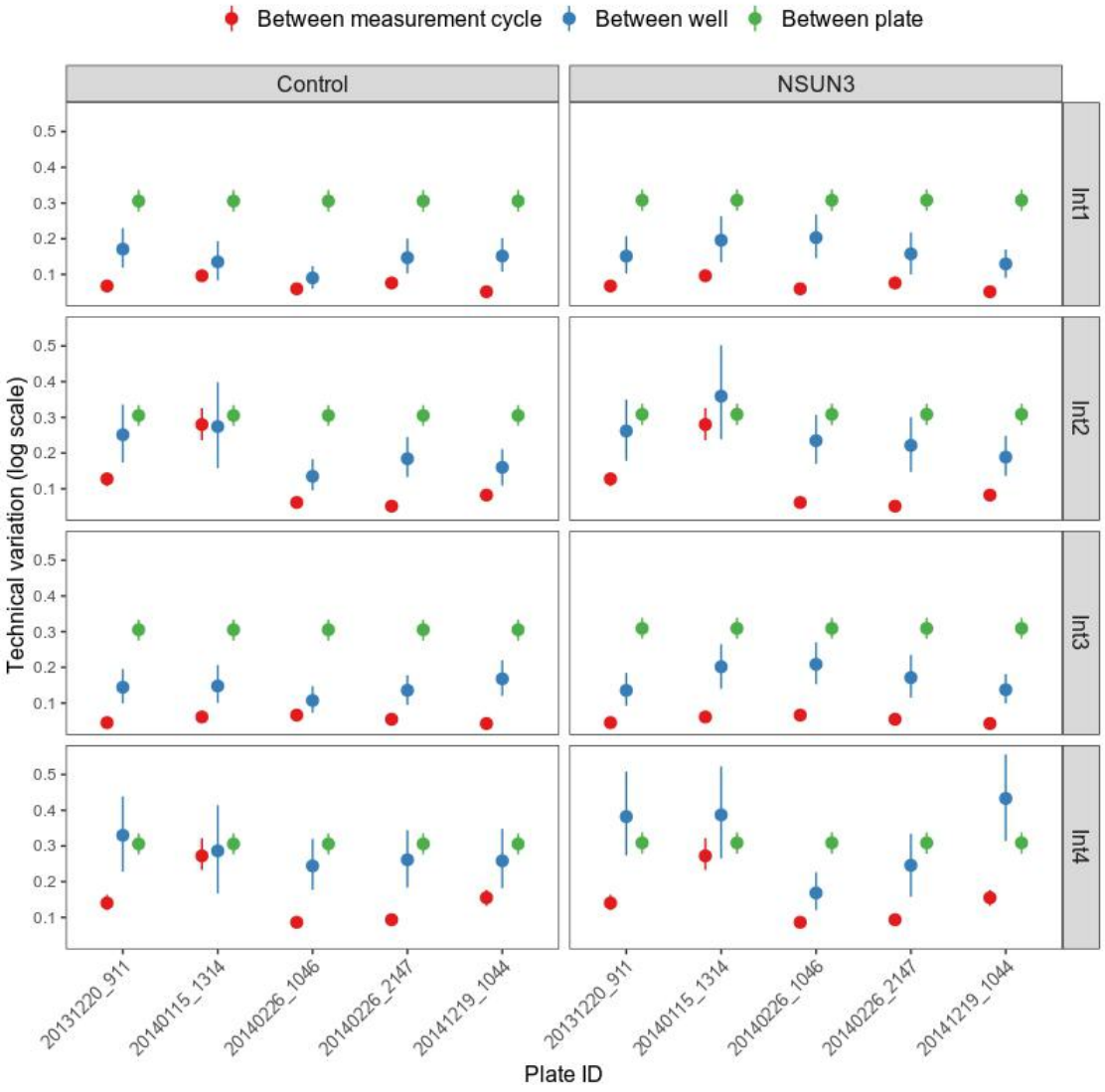

552

553 *Figure 2 Technical variations in Seahorse XF OCR data of experiments based*
554 *on the patient cell line with mutation in NSUN3 gene and the control cell*
555 *line. Int1, Int2, Int3 and Int4 represent initial, oligomycin, FCCP and*
556 *antimycin/rotenone phase. All the variations were on log scale. The dots are*
557 *the posterior mean and the line segment represent the 95% credible interval.*

558

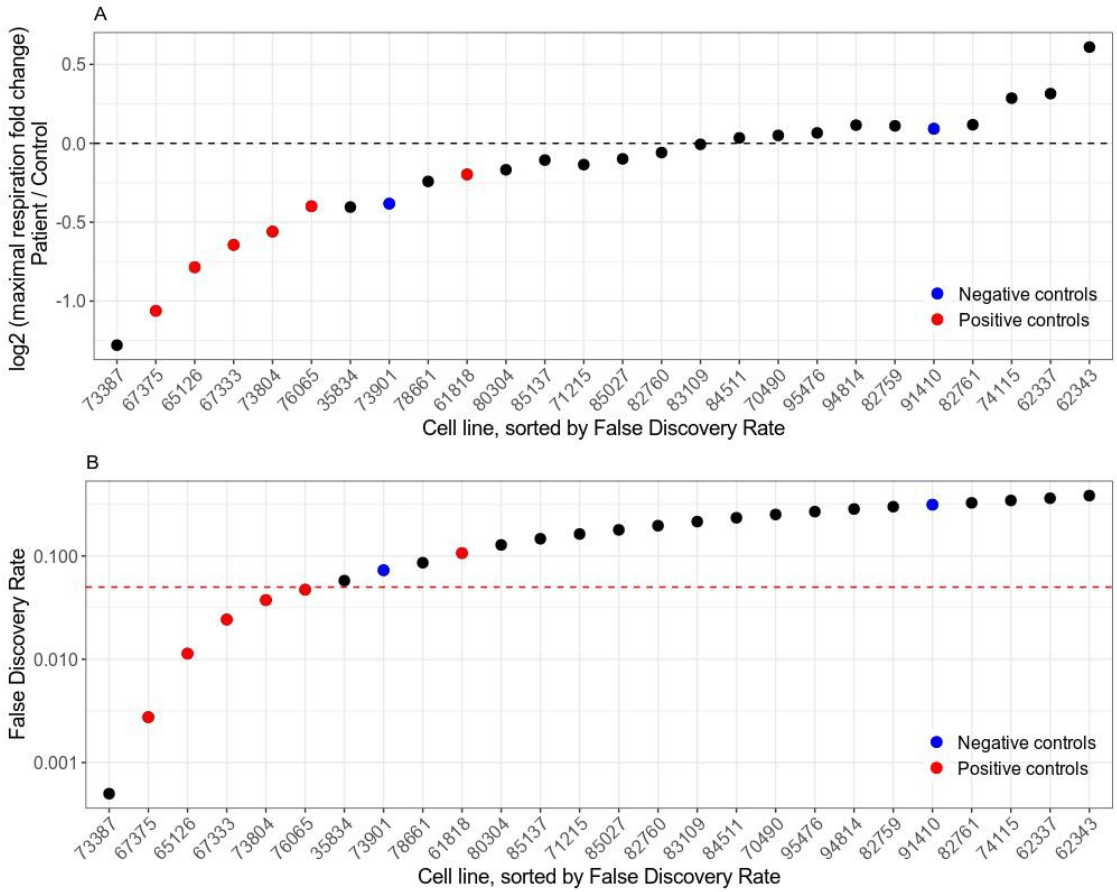

Figure 3 Maximal respiration change patient vs. control on multiple plates. (A) average log2 fold change (y-axis) of maximal respiration of all cell lines repeated across plates (x-axis) and their respective controls, sorted by the False Discovery Rate (FDR). Red and blue dots represent positive and negative controls, respectively. (B) similar to (A), but depicting FDR. Red dashed line represents FDR = 0.05.

568

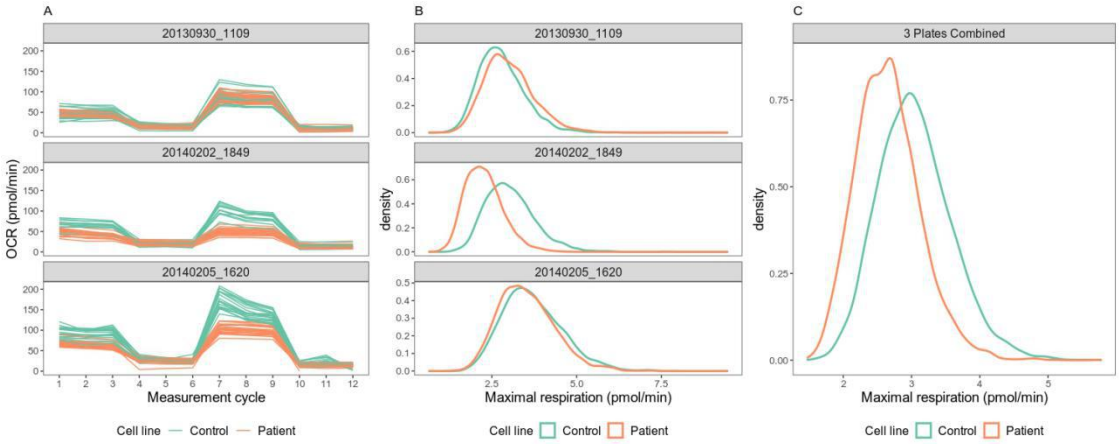

569

570 *Figure 4 (A) Raw OCR values for the cell line with genetic mutation in SFXN4*
571 *gene (patient cell line 61818) in three repeated plates. (B) Posterior*
572 *distributions of maximal respiration of the cell line with genetic mutation*
573 *in SFXN4 gene (patient cell line 61818) and the control cell line in the*
574 *same plate. (C) Posterior distributions of maximal respiration of the cell*
575 *line after combing all three repeated experiments.*

576

577

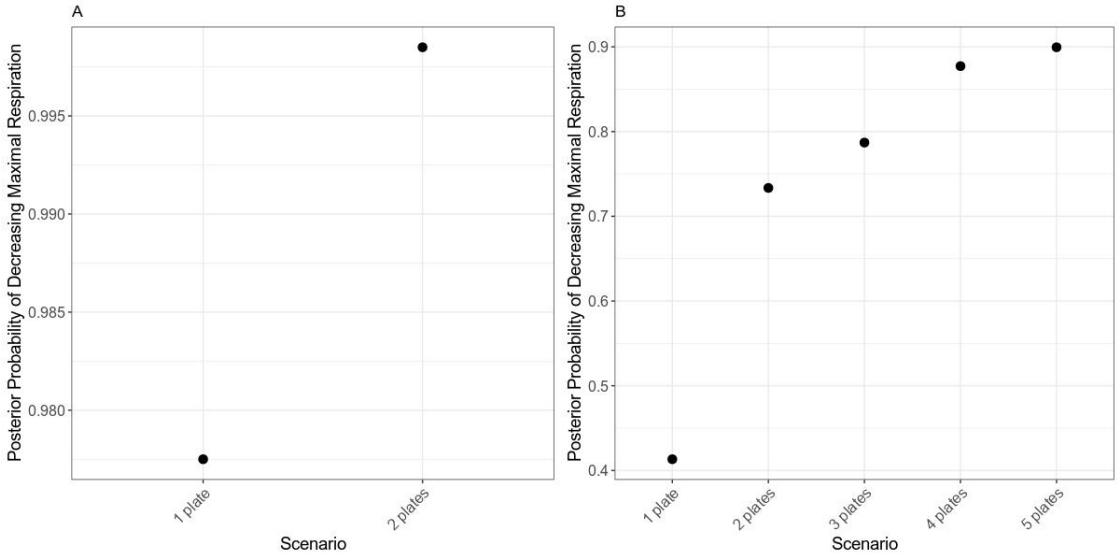

578

579 *Figure 5 (A) Posterior probability of decreasing maximal respiration in*
580 *patient cell line with mutation in PET100 gene compared to the control cell*
581 *line in the scenario with 1 or 2 plates. (B) Posterior probability of*
582 *decreasing maximal respiration in patient cell line with mutation in NUSN3*
583 *gene compared to the control cell line in the scenario with 1, 2, 3, 4 or 5*
584 *plates*